*future internet*

MDPI

*Article*

# Power-Efficient Resource Allocation for Active STAR-RIS-Aided SWIPT Communication Systems

**Chuanzhe Gao [1], Shidang Li [1,*], Yixuan Wu [2], Siyi Duan [1], Mingsheng Wei [1] and Bencheng Yu [3,*]**

[1] School of Physics and Electronic Engineering, Jiangsu Normal University, Xuzhou 221116, China; 3020214559@jsnu.edu.cn (C.G.); 2020221336@jsnu.edu.cn (S.D.); weims@jsnu.edu.cn (M.W.)
[2] SINO-RUSSIAN Institute, Jiangsu Normal University, Xuzhou 221116, China; 3020234749@jsnu.edu.cn
[3] School of Information Engineering, Xuzhou College of Industrial Technology, Xuzhou 221140, China
* Correspondence: shidangli@jsnu.edu.cn (S.L.); yubc@mail.xzcit.cn (B.Y.)

**Abstract:** Simultaneous wireless information and power transfer (SWIPT) has emerged as a pivotal technology in 6G, offering an efficient means of delivering energy to a large quantity of low-power devices while transmitting data concurrently. To address the challenges of obstructions, high path loss, and significant energy consumption associated with long-distance communication, this work introduces a novel alternating iterative optimization strategy. The proposed approach combines active simultaneous transmission and reflection of reconfigurable intelligent surfaces (STAR-RIS) with SWIPT to maximize spectrum efficiency and reduce overall system energy consumption. This method addresses the considerable energy demands inherent in SWIPT systems by focusing on reducing the power output from the base station (BS) while meeting key constraints: the communication rate for information receivers (IRs) and minimum energy levels for energy receivers (ERs). Given complex interactions between variables, the solution involves an alternating iterative optimization process. In the first stage of this approach, the passive beamforming variables are kept constant, enabling the use of semi-definite relaxation (SDR) and successive convex approximation (SCA) algorithms to optimize active beamforming variables. In the next stage, with active beamforming variables fixed, penalty-based algorithms are applied to fine-tune the passive beamforming variables. This iterative process continues, alternating between active and passive beamforming optimization, until the system converges on a stable solution. The simulation results indicated that the proposed system configuration, which leverages active STAR-RIS, achieves lower energy consumption and demonstrates improved performance compared to configurations utilizing passive RIS, active RIS, and passive STAR-RIS. This evidence suggests that the proposed approach can significantly contribute to advancing energy efficiency in 6G systems.

**Keywords:** active STAR-RIS; SWIPT; semicontinuous relaxation; penalty algorithm; alternate iterative optimization



**Citation:** Gao, C.; Li, S.; Wu, Y.; Duan, S.; Wei, M.; Yu, B. Power-Efficient Resource Allocation for Active STAR-RIS-Aided SWIPT Communication Systems. *Future Internet* **2024**, *16*, 266. https://doi.org/10.3390/fi16080266

Academic Editors: Chan Hwang See, Simeon Keates, Yousef Dama, Kelvin Anoh and Raed A. Abd-Alhameed

Received: 3 June 2024
Revised: 18 July 2024
Accepted: 24 July 2024
Published: 25 July 2024



## 1. Introduction

With the development of Internet of Things (IoT) technology, the need for ubiquitous communication between devices will become stronger [1]. Low-power devices will be employed on a large scale; however, this will lead to very high energy consumption as well as significant carbon emissions [2]. To address energy and environmental issues, SWIPT technology is expected to be an integral part of 6G [3,4]. SWIPT technology relies on wireless energy transmission technology, which allows simultaneous transmission of energy and information using the same frequency bands and waveforms in order to realize the synergy between ERs and IRs. The access point (AP) balances the energy reception and information transmission performance by optimizing the energy beamforming and information beamforming. However, the transmission efficiency and range of the SWIPT system are not ideal for long-distance transmission due to the fact that the energy and

information emission are concentrated at the AP, and the path loss is high when the receiver is in the shadow area of the obstacle.

With the aim of decreasing the SWIPT system's energy use, researchers have conducted research on full-duplex technology [5] and reconfigurable intelligent surface (RIS). A lot of reflective unit elements are distributed on the RIS plane, and the amplitude and direction of incoming signal can be adjusted by changing phase or amplitude parameters of units through coding control of circuits such as programmable gate arrays, thus expanding the coverage of the signal [6]. Therefore, the use of RIS can alleviate the problem of transmission loss caused by long-distance communication in SWIPT systems.

A great deal of research has been conducted by scholars on passive RIS-assisted SWIPT techniques. One study [7] explored the simultaneous optimization of message rate and received power in passive RIS-assisted multi-input single-output downlink multi-user wireless networks and developed a practical algorithm. Another study [8] addressed the challenge of low far-field power transmission efficiency with a passive RIS-assisted SWIPT system. Utilizing sorting and iterative optimization algorithms, it sought to maximize the minimum rate for information receivers, both in ideal and non-ideal channels. In one study [9], passive RIS was employed to enhance the performance of cooperative non-orthogonal multiple access (C-NOMA). The objective was to maximize the data rate for cell-edge users while considering the energy constraints and minimum data rate requirements of cell-center users. Another study [10] presented the problem of maximum average secrecy rate, using RIS to enhance physical layer security in Rayleigh fading channels. One study [11] combined RIS with UAVs to simultaneously transmit information and collect energy by segmenting passive reflective arrays in geometric space, ensuring quality of service in dynamic wireless environments. A further study [12] investigated the deep integration of RIS and NOMA, which dramatically increased the data transfer rate in the Internet of Medical Things (IOMT) while significantly improving the safety of private users in RIS-assisted NOMA networks. These findings suggest that the RIS-assisted SWIPT system is able to further boost wireless system capability.

However, to further decrease the power consumption and improve the performance of the system, active RIS has been widely used [13]. One study [14] proposed an active RIS-assisted SWIPT system to maximize the rate of IRs. The research results indicated that an active RIS-assisted SWIPT system can obtain superior performance gains compared to other systems. Another study [15] explored the issue of active RIS-assisted multi-user downlink transmission and rate maximization based on actual hardware impairments. The simulation results showed that active RIS achieves a higher total transmission rate compared to passive RIS. One study [16] investigated an algorithm for combined emission beamforming and energy-containing RIS reflection matrices to maximize energy efficiency using quadratic transform-based fractional order planning techniques. A different study [17] examined the complex and non-convex robust secrecy rate optimization problem when AP and RIS share identical power source. The research findings indicated that, in the context of active RIS, the proposed algorithm delivers superior secrecy rate performance in contrast to passive RIS. Another study [18] addressed the problem of limited performance gain of conventional passive RIS by proposing an active RIS-assisted multi-user multiple-input multiple-output SWIPT system, which achieved the system power minimization while satisfying the minimum communication rate demand and energy collection constraints of both the IRs and ERs.

However, both passive and active RIS only consider the case of reflection and not transmission. The tunable components are integrated into the substrate of the RIS, and the wireless signal cannot penetrate the RIS, allowing no energy leakage into the space behind the RIS; therefore, the AP and users must be placed on identical side of RIS, resulting in utilization of only a half-space intelligent radio environment with very limited spectrum of space utilization, severely limiting the flexibility and effectiveness of the RIS. To overcome the limitations of RIS and thus make fuller use of spectrum resources, researchers have proposed a new concept—STAR-RIS, which is not only reflective but also transmissive

compared to RIS, thus achieving 360° wireless coverage [19]. One study [20] investigated a multi-input single-output passive STAR-RIS-assisted NOMA downlink network, achieving maximum energy efficiency while balancing total rate and power consumption. A different study [21] proposed a network of passive STAR-RIS-assisted SWIPT systems applying the time switching (TS) protocol to maximize the total rate of all the information receivers by co-optimizing energy allocation of IRs and the beamforming vectors of passive STAR-RIS. Zhu investigated the max–min fairness optimization problem for SWIPT systems with assistance of passive STAR-RIS in imperfect channel states under the constraints of the signal-to-interference-plus-noise Ratio (SINR) of IRs, aiming to maximize the minimum power collected by the ERs [22].

Although the above work has achieved good results in passive RIS, active RIS, and passive STAR-RIS-assisted SWIPT systems, respectively, passive RIS-assisted SWIPT systems still have high power consumption due to signal fading issues, and passive RIS is only reflective but not transmissive, resulting in limited spectrum space utilization. Although active RIS can reduce the attenuation by amplifying the signal, it still does not have the function of transmission, and although passive STAR-RIS has the function of transmission and reflection, it cannot amplify the signal; therefore, an active STAR-RIS that combines signal amplification, transmission, and reflection to reduce the AP transmitting power to a greater extent has become a hotspot in current research. However, few existing studies involve the combination of active STAR-RIS and SWIPT techniques. To solve this issue, the present paper explores the problem of energy minimization in an active STAR-RIS assisted SWIPT system. The contributions of this paper are as below:

- This paper constructs a SWIPT system model assisted by active STAR-RIS and consisting of AP, active STAR-RIS, multiple IRs, and multiple ERs. With multiple ERs located in the reflective space and multiple IRs located in the transmissive space, our goal is to minimize the AP transmission power constrained by communication rate of IRs and the energy accepted by the smallest ERs so that the spectrum resources of the whole communication network are fully utilized with the optimal energy transmission performance;
- To tackle the non-convex nature of the problem, this paper proposes an alternating optimization (AO) algorithm for active and passive beamforming variable assignment. The approach involves two subproblems: In the first, passive beamforming variables are fixed, and the active beamforming variables are optimized using semi-definite relaxation (SDR) and successive convex approximation (SCA). In the second subproblem, active beamforming variables are kept constant, and a penalty-based algorithm is used to optimize the passive beamforming variables. By alternating between these two subproblems, the algorithm converges on an optimal solution despite the problem's non-convexity;
- The simulation results show that the proposed joint iterative optimization method converges rapidly and delivers high-quality results. With active STAR-RIS, system performance significantly improves, making better use of spectrum resources. Comparing four system models, namely active/passive RIS and active/passive STAR-RIS, the active STAR-RIS-assisted SWIPT system achieved minimal AP transmit power and superior performance even with consistent variables like SINR, the quantity of active STAR-RIS reflector units, the quantity of AP transmitting antennas, and minimum-energy receiver power. Active STAR-RIS also allows the system to utilize both reflective and transmissive spaces, maximizing spectrum resource efficiency. This dual-mode capability contributes to enhanced communication and energy transfer.

The paper is organized as follows: Section 2 mainly introduces the system model of this paper and addresses the issue of minimum AP transmit power; in Section 3, the subproblems 1 and 2 are solved using the SDR algorithm and the penalty algorithm, respectively, and the optimization algorithm is employed with alternating iterations until the system converges; Section 4 mainly introduces the analysis of the simulation results. The whole paper is summarized in Section 5.

The acronyms used in this paper are shown in Table 1.

**Table 1.** Abbreviations used in this paper.

| Acronyms | Full Name |
|---|---|
| SWIPT | Simultaneous Wireless Information and Power Transfer |
| AP | Access Point |
| SDR | Semi-Definite Relaxation |
| SCA | Successive Convex Approximation |
| IoT | Internet of Things |
| RIS | Reconfigurable Intelligent Surface |
| NOMA | Non-Orthogonal Multiple Access |
| BS | Base Station |
| AO | Alternating Optimization |
| SINR | Signal-to-Interference-plus-Noise Ratio |
| TS | Time Switching |
| IRs | Information Receivers |
| ERs | Energy Receivers |

## 2. System Model and Problem Description

### *2.1. System Model*

Figure 1 illustrates the system model studied in this paper. We studied a narrowband active STAR-RIS-assisted SWIPT system that operates on a frequency flat channel. Here, the AP of $N$ antennas serves IRs and ERs assisted by an active STAR-RIS containing $M$ units. $K_I = \{1, 2, ..., k_I\}$ and $K_E = \{1, 2, ..., k_E\}$ represent IRs and ERs, respectively. Assuming that obstacles block the direct communication link between the AP and users, the deployed active STAR-RIS provides communication services and meets the energy-harvesting requirements for users in signal-blind areas by reflecting and transmitting signals. $G \in \mathbb{C}^{M \times N}$, $f_{t,i}^H \in \mathbb{C}^{1 \times M}$, and $f_{r,j}^H \in \mathbb{C}^{1 \times M}$ represent channels from AP to the active STAR-RIS, active STAR-RIS to $i$-th IRs, and active STAR-RIS to $j$-th ERs, respectively. For simplicity, linear transmission precoding is considered at the AP, and it is assumed that each information receiver or energy receiver is allocated a separate information or energy beam.

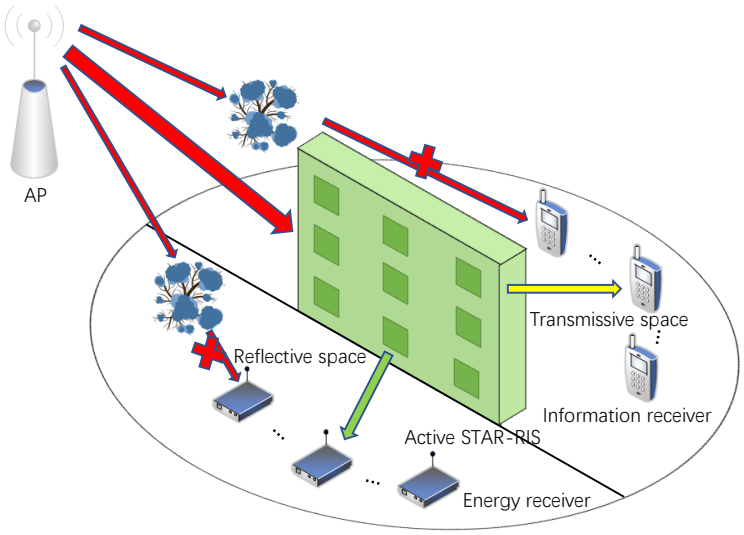


**Figure 1.** Active STAR-IRS-assisted SWIPT system model.

### *2.2. Problem Description*

Let $s_m$ represent the signal incoming onto the $m$-th unit of the active STAR-RIS, where $m \in \overline{\mathrm{M}} \triangleq 1, 2, ..., M$. $t_m = (\sqrt{\beta_m^t} e^{j\theta_m^t}) s_m$ and $r_m = (\sqrt{\beta_m^r} e^{j\theta_m^r}) s_m$ represent trans-

mitted and reflected signals on the $m$-th unit, respectively, where $\sqrt{\beta_m^t} \in [0, \sqrt{\beta_{\max}}]$, $\sqrt{\beta_m^r} \in [0, \sqrt{\beta_{\max}}]$, $\theta_m^t \in [0, 2\pi)$, $\theta_m^r \in [0, 2\pi)$, and $\beta_{\max} \geq 1$. The variable $\beta_m^t$ and $\beta_m^r$ must meet the following conditions:

$$\beta_m^t + \beta_m^r \leq \beta_{\max}, \forall m \in \overline{\mathrm{M}} \tag{1}$$

This paper focuses on the energy splitting (ES) protocol for active STAR-RIS: For ES mode, it is assumed that all units of active STAR-RIS operate in reflection and transmission modes, and the signal on each unit is decomposed into an emission signal and reflection signal. The decomposition ratio is $\beta_m^t : \beta_m^r$. $\Theta_t^{\mathrm{ES}} = \mathrm{diag}\left(\sqrt{\beta_1^t} e^{j\theta_1^t}, \sqrt{\beta_2^t} e^{j\theta_2^t}, ..., \sqrt{\beta_M^t} e^{j\theta_M^t}\right)$ and $\Theta_r^{\mathrm{ES}} = \mathrm{diag}\left(\sqrt{\beta_1^r} e^{j\theta_1^r}, \sqrt{\beta_2^r} e^{j\theta_2^r}, ..., \sqrt{\beta_M^r} e^{j\theta_M^r}\right)$ represent the emission and reflection coefficient array, respectively.

Let $x_i^I$, $x_j^E$ denote the signals carrying information and carrying energy, respectively, where $i \in K_I$, and $j \in K_E$. The accepted signal at the $i$-th IRs is as follows:

$$y_i^{\mathrm{ES}} = f_{t,i}^H P \Theta_t^{\mathrm{ES}} G \left( \sum_{i \in K_I} w_i x_i^I + \sum_{j \in K_E} v_j x_j^E \right) + f_{t,i}^H P n_{RIS} + n_i \tag{2}$$

where $w_i \in \mathbb{C}^{N \times 1}$, $v_j \in \mathbb{C}^{N \times 1}$ are the precoding vectors of the $i$-th IRs and the $j$-th ERs, respectively. For information signals $x_i^I$, there are $x_i^I \sim CN(0,1)$, $E(\left| x_j^E \right|_2) = 1$ and $\forall i \in K_I, \forall j \in K_E$. In Equation (2), there are $n_i \sim CN(0, \sigma_i^2)$, $P \triangleq \{P_1, P_2, ..., P_M\}^H$, and $n_{RIS} \sim CN(0, \sigma_{RIS}^2)$.

Since energy beams are pseudo-random signals that do not carry any information, their waveforms are assumed to be known at the AP and at each information receiver prior to data transmission, and it is assumed in this paper that the interference they cause can be cancelled out at each information receiver. Therefore, for the ES protocol, the communication rate achievable by the $i$-th information receiver is as follows:

$$R_i^{\mathrm{ES}} = lb \left( 1 + \frac{\left| f_{t,i}^H P \Theta_t^{\mathrm{ES}} G w_i \right|^2}{\sum\limits_{j \neq i, j \in K_I} \left| f_{t,i}^H P \Theta_t^{\mathrm{ES}} G w_j \right|_2 + \left| \left| f_{t,i}^H P \Theta_t^{\mathrm{ES}} \right| \right|_2 \sigma_{RIS}^2 + \sigma_i^2} \right) \tag{3}$$

If the noise power is ignored, the power is accepted at the $j$-th energy receiver:

$$E_j^{\mathrm{ES}} = \sum_{k \in K_I} \left| f_{r,j}^H P \Theta_r^{\mathrm{ES}} G w_k \right|^2 + \sum_{k \in K_E} \left| f_{r,j}^H P \Theta_r^{\mathrm{ES}} G v_k \right|^2, \forall j \in K_E \tag{4}$$

The objective of this paper is the joint optimization of the active beamforming variable $\{w_i, v_j\}$, the passive beamforming variable $\Theta_k^{\mathrm{ES}}, \forall k \in \{t, r\}$, and the amplification multiplier matrix $P$ for a given ES operation protocol under the communication rate of the information receiver and the energy-harvesting constraints of the energy receiver so as to minimize the AP power consumption. The optimization problem can be thus stated:

$$\min_{\{w_i\}, \{v_j\}, \Theta_k^{\mathrm{ES}}} \sum_{i \in K_I} ||w_i||^2 + \sum_{j \in K_E} ||v_j||^2 \tag{5}$$

$$s.t. \ R_i^{\mathrm{ES}} \geq \overline{R}_i, \forall i \in K_I \tag{6}$$

$$E_j^{\mathrm{ES}} \geq \overline{E}_j, \forall j \in K_E \tag{7}$$

$$\Theta_k^{\mathrm{ES}} \in \mathbb{F}^{\mathrm{ES}}, \forall k \in \{t, r\} \tag{8}$$

where $\overline{R}_i$ in Equation (6) denotes the minimum rate requirement for user $i$, $\overline{E}_j$ in Equation (7) denotes the minimum energy harvesting requirement for user $j$, and $\mathbb{F}^{\mathrm{ES}}$ in Equation (8) denotes the feasible set corresponding to the emission and reflection coefficient matrix.

Because of the coupling between variables, this paper uses the algorithm of alternating iteration to optimize the solution for different variables. We first stabilize the passive beamforming variable $\Theta_k^{\mathrm{ES}}, \forall k \in \{t, r\}$ and the magnification matrix $P$, optimizing variable $\{w_i, v_j\}$. Once the most optimal solution of $\{w_i, v_j\}$ is available, we fix the value unchanged and then optimize the passive beamforming variable $\Theta_k^{\mathrm{ES}}, \forall k \in \{t, r\}$ and magnification matrix $P$ and so on iteratively until the system converges.

## 3. Optimization of Algorithm Design

In this paper, alternating optimization method is used to address joint beamforming optimization problem. That is, problem (5) is split into two sub-problems: For the first, SDR method is used to optimize $\{w_i, v_j\}$ given $Q_k = P\Theta_k^{\mathrm{ES}}, k \in \{t, r\}$, and for the second, the penalty-based algorithm is used to optimize $\{w_i, v_j\}$ given $Q_k$.

### *3.1. Active Beamforming Optimisation*

First, we consider the optimization of $\{w_i, v_j\}$ given $Q_k, k \in \{t, r\}$. Let $h_{t,i}^H = f_{t,i}^H Q_t G$ and $h_{r,j}^H = f_{r,j}^H Q_r G$ define $H_{t,i} = h_{t,i} h_{t,i}^H, H_{r,j} = h_{r,j} h_{r,j}^H, W_i = w_i w_i^H, \forall i \in K_I$ and meet $W_i \succeq 0, rank(W_i) = 1$. Let $V_j = v_j v_j^H, \forall j \in K_E$ meet $V_j \succeq 0, rank(V_j) = 1$. Problem (5) is converted into the optimization problem below:

$$\min_{W_i, V_j} \sum_{i \in K_I} \mathrm{TR}(W_i) + \sum_{j \in K_E} \mathrm{TR}(V_j) \tag{9}$$

$$s.t.\ \overline{\Upsilon}_i \sum_{\bar{i} \neq i, \bar{i} \in K_I} \mathrm{TR}(H_{t,i} W_i) - \mathrm{TR}(H_{t,i} W_i) + ||f_{t,i}^H Q_t||^2 \overline{\Upsilon}_i \sigma_{RIS}^2 + \overline{\Upsilon}_i \sigma_i^2 \leq 0, \forall i \in K_I \tag{10}$$

$$\sum_{k \in K_E} \mathrm{TR}(H_{r,j} V_k) + \sum_{k \in K_I} \mathrm{TR}(H_{r,j} W_k) \geq \overline{E}_j, \forall j \in K_E \tag{11}$$

$$rank(W_i) = 1, rank(V_j) = 1 \tag{12}$$

$$W_i \succeq 0, V_j \succeq 0, \forall i \in K_I, \forall j \in K_E \tag{13}$$

In the above equation $\overline{\Upsilon}_i = 2^{\overline{R}_i} - 1$, because problem (9) has a non-convex constraint (12), to address this problem, this paper uses the SDR method, and neglecting (12), problem (9) is transformed into the following semidefinite relaxation form (14).

$$\min_{W_i, V_j} \sum_{i \in \kappa_I} \mathrm{TR}(W_i) + \sum_{j \in \kappa_\varepsilon} \mathrm{TR}(V_j) \tag{14}$$

$$s.t.\ \overline{\Upsilon}_i \sum_{\bar{i} \neq i, \bar{i} \in K_I} \mathrm{TR}(H_{t,i} W_i) - \mathrm{TR}(H_{t,i} W_i) + ||f_{t,i}^H Q_t||^2 \overline{\Upsilon}_i \sigma_{RIS}^2 + \overline{\Upsilon}_i \sigma_i^2 \leq 0, \forall i \in K_I \tag{15}$$

$$\sum_{k \in K_E} \mathrm{TR}(H_{r,j} V_k) + \sum_{k \in K_I} \mathrm{TR}(H_{r,j} W_k) \geq \overline{E}_j, \forall j \in K_E \tag{16}$$

$$W_i \succeq 0, V_j \succeq 0, \forall i \in K_I, \forall j \in K_E \tag{17}$$

The relaxation problem (14) is a convex positive semidefinite programming problem, which can be effectively solved by using standard convex optimization tools such as CVX. Next, the compactness of rank constraint relaxation in (12) was studied.

**Theorem 1.** *Problem (14) always satisfies* $rank(W_i) = 1, rank(V_j) = 1, \forall i \in K_I, \forall j \in K_E$ *without losing optimality.*

**Proof of Theorem 1.** Detailed proof can be found in Appendix A. □

*3.2. Passive Beamforming Optimization*

Secondly, we consider the optimization of $Q_k, k \in \{t, r\}$ given $\{w_i, v_j\}$ and define $c_{t,i} = \text{diag}(f_{t,i}^H)Gw_i$, $c_{r,j} = \text{diag}(f_{r,j}^H)Gv_j$. We also define the vector of transmission and reflection coefficients as $q_k = [P_1\sqrt{\beta_1^k}e^{j\theta_1^k}, P_2\sqrt{\beta_2^k}e^{j\theta_2^k}, ..., P_M\sqrt{\beta_M^k}e^{j\theta_M^k}]^H, \forall k \in \{t, r\}$. Let $C_{t,i} = c_{t,i}c_{t,i}^H, C_{r,j} = c_{r,j}c_{r,j}^H, Q_k = q_k(q_k)^H, \forall k \in \{t, r\}$ meet $Q_k \succeq 0$, $diag(Q_k) = \beta^k$, $rank(Q_k) = 1$, where $\beta^k \triangleq [P_1^2\beta_1^k, P_2^2\beta_2^k, ..., P_M^2\beta_M^k], \forall k \in \{t, r\}$.

The problem is next solved using a penalty-based algorithm. We transform problem (5) into the following optimization problem:

$$\min_{Q_k, \beta_k} \eta \sum_{k \in \{t,r\}} (||Q_k||_* - ||Q_k||_2) \tag{18}$$

$$\begin{aligned} s.t. \ \overline{Y}_i \sum_{\tilde{i} \neq i, \tilde{i} \in K_I} \text{TR}(C_{t,\tilde{i}}Q_t) - \text{TR}(C_{t,i}Q_t) + ||f_{t,i}^H Q_t||^2 \overline{Y}_i \sigma_{RIS}^2 \\ + \overline{Y}_i \sigma_i^2 \leq 0, \forall i \in K_I \end{aligned} \tag{19}$$

$$\sum_{k \in K_E} \text{TR}(C_{r,j}Q_r) + \sum_{k \in K_I} \text{TR}(C_{r,j}Q_r) \geq \overline{E}_j, \forall j \in K_E \tag{20}$$

$$diag(Q_k) = \beta^k, \forall k \in \{t, r\} \tag{21}$$

$$Q_k \succeq 0, \forall k \in \{t, r\} \tag{22}$$

$$0 \leq \beta_m^t, \beta_m^r \leq \beta_{\max}, \ \beta_m^t + \beta_m^r \leq \beta_{\max}, \forall m \in \overline{M} \tag{23}$$

where the nonconvex rank-one constraint $rank(Q_k) = 1$ is equivalently written as an equational constraint:

$$||Q_k||_* - ||Q_k||_2 = 0, \forall k \in \{t, r\} \tag{24}$$

We next relax the equation constraint (24) to a penalty item attached to the target function. In Equation (24), there are $||Q_k||_* = \sum_i \sigma_i(Q_k)$ and $||Q_k||_2 = \sigma_i(Q_k)$ standing for the nuclear and spectral paradigms, respectively, and $\sigma_i(Q_k)$ is the $i$-th greatest singular value of array $Q_k$. For arbitrary Ermitian matrices $Q_k \in \overline{H}^M, Q_k \succeq 0$, there will always be $||Q_k||_* - ||Q_k||_2 \geq 0$. The equation holds true only when the rank of $Q_k$ is 1.

When the $Q_k$ rank is not one, $\eta > 0$ is the penalty factor of target function. A small value is first used to initialize $\eta$ to find a feasible point, after which the iterative process gradually increases $\eta$ to a value enormous enough to ultimately obtain a practicable rank-one solution. The algorithm ends when the following situations occur:

$$\max\{||Q_k||_* - ||Q_k||_2, \forall k \in \{t, r\}\} \leq \varepsilon_1 \tag{25}$$

where $\varepsilon_1$ denotes the accuracy that satisfies the predefined constraints of the equation. For any penalty factor $\eta > 0$, problem (18) remains nonconvex due to the nonconvexity of the target function. It is converted to (26) using the SCA method below.

For a given point $Q_k^{(n)}$, a convex upper boundary for the penalty item is gained using a first-order Taylor expansion during the $n$-th iteration process:

$$\left|\left|Q_k\right|\right|_* - \left|\left|Q_k\right|\right|_2 \leq \left|\left|Q_k\right|\right|_* - \overline{Q}_k^{(n)} \tag{26}$$

where $\overline{Q}_k^{(n)} \triangleq \left|\left|Q_k^{(n)}\right|\right|_2 + \text{TR}[\overline{u}(Q_k^{(n)})(\overline{u}(Q_k^{(n)}))^H(Q_k - Q_k^{(n)})]$, $\overline{u}(Q_k^{(n)})$ is the eigenvector corresponding to the largest eigenvalue of $Q_k^{(n)}$.

Thus, problem (18) transforms into the following optimization problem:

$$\min_{Q_k,\beta_k} \eta \sum_{k\in\{t,r\}} (\left|\left|Q_k\right|\right|_* - \overline{Q}_k^{(n)}) \tag{27}$$

$$s.t.\ \overline{\Upsilon}_i \sum_{\bar{i}\neq i,\bar{i}\in K_I} \mathrm{TR}(C_{t,\bar{i}}Q_t) - \mathrm{TR}(C_{t,i}Q_t) + ||f_{t,i}^H Q_t||^2 \overline{\Upsilon}_i \sigma_{RIS}^2 + \overline{\Upsilon}_i \sigma_i^2 \leq 0, \forall i \in K_I \tag{28}$$

$$\sum_{k\in K_E} \mathrm{TR}(C_{r,j}Q_r) + \sum_{k\in K_I} \mathrm{TR}(C_{r,j}Q_r) \geq \overline{E}_j, \forall j \in K_E \tag{29}$$

$$diag(Q_k) = \beta^k, \forall k \in \{t,r\} \tag{30}$$

$$Q_k \succeq 0, \forall k \in \{t,r\} \tag{31}$$

$$0 \leq \beta_m^t, \beta_m^r \leq \beta_{\max}, \beta_m^t + \beta_m^r \leq \beta_{\max}, \forall m \in \overline{M} \tag{32}$$

However, although the optimization problem (27) includes a target function, it still confronts availability issues since arbitrary $Q_k$ that meets the constraints is an optimum solution, so we mandatorily carry out a solution that optimizes the value of the SINR and the collected energy and at the same time satisfies the rank-one constraints [23], and in order to achieve, this we propose a new slack variable $\tau_i$ as the "SINR residuals", and the new problem is given by Equation (33):

$$\min_{Q_k,\beta_k} \eta \sum_{k\in\{t,r\}} (\left|\left|Q_k\right|\right|_* - \overline{Q}_k^{(n)}) - \sum_{i=1}^{K_I} \alpha\tau_i \tag{33}$$

$$s.t.\ (\overline{\Upsilon}_i + \tau_i) \sum_{\bar{i}\neq i,\bar{i}\in K_I} \mathrm{TR}(C_{t,\bar{i}}Q_t) - \mathrm{TR}(C_{t,i}Q_t) + ||f_{t,i}^H Q_t||^2 (\overline{\Upsilon}_i + \tau_i)\sigma_{RIS}^2 + (\overline{\Upsilon}_i + \tau_i)\sigma_i^2 \leq 0, \forall i \in K_I \tag{34}$$

$$\sum_{k\in K_E} \mathrm{TR}(C_{r,j}Q_r) + \sum_{k\in K_I} \mathrm{TR}(C_{r,j}Q_r) \geq \overline{E}_j, \forall j \in K_E \tag{35}$$

$$diag(Q_k) = \beta^k, \forall k \in \{t,r\} \tag{36}$$

$$Q_k \succeq 0, \forall k \in \{t,r\} \tag{37}$$

$$0 \leq \beta_m^t, \beta_m^r \leq \beta_{\max}, \beta_m^t + \beta_m^r \leq \beta_{\max}, \forall m \in \overline{M} \tag{38}$$

$$\alpha, \tau_i \geq 0, \forall i \tag{39}$$

The optimization problem (33) has the same feasible set as the optimization problem (27); however, the optimization problem (33) has better convergence.

For the optimization problem (33), if $Q$ is rank one, then the solution of $Q^*$ is also optimal for problem (33). In this case, by performing an eigenvalue decomposition on $Q^*$, the corresponding $q^*$ can be obtained. $\overline{q}_{\max}$ denotes the unit eigenvector associated with the largest eigenvalue $\lambda_{\max}(Q)$. The optimal reflection vector $\overline{q} = \sqrt{\lambda_{\max}(Q)}\overline{q}_{\max}$ can be obtained. Finally, the most optimal solution $q^*$ can be represented as $q^* = [\overline{q}/\overline{q}_{M+1}]_{(1:M)}$. Otherwise, if $Q^*$ has a higher rank, a further rank 1 solution needs to be constructed as follows. The eigenvalue decomposition of $Q^*$ is expressed as $Q^* = U_Q \sum_Q U_Q^H$, where $U_Q$ is unitary, and $\sum_Q$ is diagonal. $q^* = U_Q \sum_Q^{\frac{1}{2}} r$ is then set, where $r \sim CN(0 \sim I)$. Thus, the solution to problem (33) is $q^* = [\overline{q}/\overline{q}_{M+1}]_{(1:M)}$. Finally, the solutions of the obtained problems (14) and (33) are used to solve the problem (5) through alternate optimization, in which problems (14) and (33) are solved in an alternating manner until convergence.

### *3.3. Complexity Analysis*

Following the AO framework, problem (5) can be solved by solving problems (14) and (33) in an iterative manner. It can be observed that these resulting convex problems contain linear constraints; thus, all problems can be solved by the interior point method [24]. Specifically, by ignoring the non-dominated linear constraints, the general expression for complexity is provided in [25]. Then, the complexity of solving problems (14) and (33) is given by $O_{\mathrm{F}} = O(M^{3.5}N^{4.5})$ and $O_{\mathrm{U}} = O(M^{4.5}N^{3.5})$, respectively. Furthermore, let $I_{iter}$ denote the number of iterations needed for the convergence of the proposed AO algorithm; the overall complexity is given by $O(I_{iter}(O_{\mathrm{F}} + O_{\mathrm{U}}))$.

### *3.4. Algorithm Design*

Because of complex interactions between the variables, problem (5) cannot be solved directly, so it is necessary to fix the passive beamforming variables first, then solve the problem (14), find the optimal solution of the active beamforming variables, fix the solution, and then solve the problem (33) so as to continuously iterate until the system converges. In Algorithm 1, the process of penalty-based algorithms is summarized. Firstly, the feasible points and penalty factors are initialized. After obtaining the optimal solution to problem (33), the penalty factors are updated and stopped after reaching the max iteration count or falling below the predetermined threshold. In Algorithm 2, the AO method is summarized. Firstly, the feasible points are initialized; after the variables $w^{(r+1)}$ and $v^{(r+1)}$ are obtained, the variables $Q^{(r+1)}$ are obtained by Algorithm 1 so as to continuously optimize until the maximum quantity of iterations or the difference between two objective function values is lower than the predetermined threshold.

**Algorithm 1:** Solving problems (33) based on penalty algorithms

1: Initializing feasible points: $\left\{Q_k^{(0)}\right\}$, penalty factor $\eta$
2: repeatable cycle:
3: Setting the loop iteration count $n = 0$
4: update $\left\{Q_k^{(n+1)}\right\}$, by solving problems (33), $n = n + 1$
5: update $\eta = \omega\eta$
6: Reach the maximum quantity of iterations $n_{\max}$ or constraint violation below predetermined threshold $\varepsilon_1 > 0$, terminate
7: Recovery of $q^*$ from $Q^*$

**Algorithm 2:** Solving problem (5) based on alternating optimization algorithm

1: Initializing feasible points: $Q^{(0)}$
2: repeatable cycle:
3: Setting the loop iteration index $r = 0$
4: For a given $Q_k^{(r)}$, $w^{(r+1)}$ and $v^{(r+1)}$ are obtained by solving problem (14) using CVX
5: After obtaining $w^{(r+1)}$ and $v^{(r+1)}$, find the solution of problem (33) to obtain $Q^{(r+1)} = diag(q^{n+1})$ and $r = r + 1$ by using Algorithm 1.
6: Reached the maximum quantity of iterations $r_{\max}$, or difference between objective function values between two iterations is lower than the predetermined threshold $\varepsilon_2 > 0$, end

## 4. Simulation Analysis

Figure 2 shows the simulation model under consideration. The AP and active STAR-RIS are placed in $(0, 0, 0)$ m and $(0, 10, 0)$ m, respectively. The direct view link from the AP to IRs and ERs is obstructed by obstacles. A semicircular area, centered on the active STAR-RIS, randomly hosts a multitude IRs and ERs situated at radii of $d_r = 2$ m and $d_t = 20$ m, respectively. The number of Monte Carlo simulations refers to the number of times the actual results are approximated through multiple experiments. As the number of Monte Carlo simulations increases, the estimated values gradually converge to the true values. The more Monte Carlo simulations there are, the closer the estimated results are to the true

values and the higher the accuracy. The common number of Monte Carlo simulations is set to 200 [26,27], 500 [28], 1000 [29–31], 2000 [32], and 100,000 [33]. However, although a small number of Monte Carlo simulations can obtain partially smooth curves, there are also some curves that are not smooth. Excessive Monte Carlo simulations can obtain smoother experimental results, but they consume a lot of time, while 1000 Monte Carlo simulations can obtain smoother experimental results and consume less time. Therefore, this paper sets the number of Monte Carlo simulations to 1000.

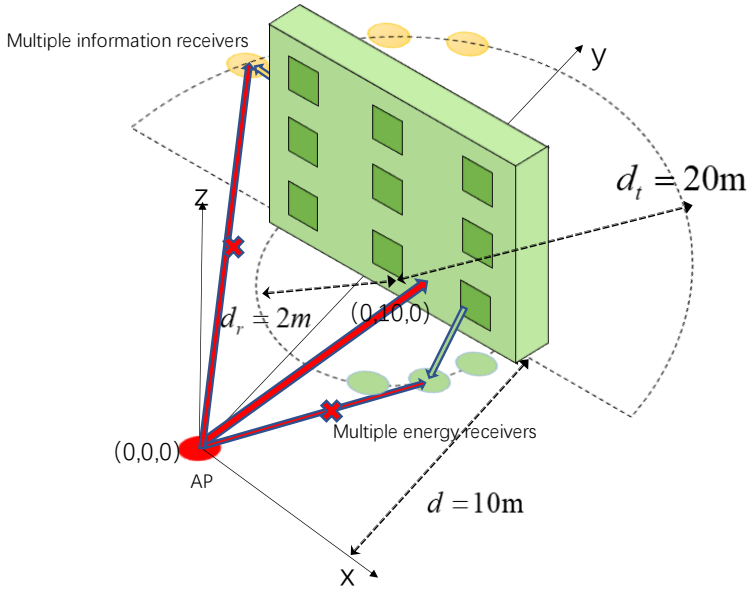


**Figure 2.** System Simulation Model.

For channel $G$, the model is as follows:

$$G = \sqrt{\frac{\rho_0}{d_{AR}^{\alpha_{AR}}}}\left(\sqrt{\frac{K_{AR}}{K_{AR}+1}}G^{LOS} + \sqrt{\frac{1}{K_{AR}+1}}G^{NLOS}\right) \tag{40}$$

The Rice factor is $K_{AR} = 3$ dB; $\alpha_{AR}$ represents the corresponding path loss index. The unit path loss is $\rho_0 = 30$ dB. $G^{LOS}$ is deterministic line-of-sight component, $G^{NLOS}$ is a random non-line-of-sight component, and other channels can be obtained using similar methods.

The other required parameter settings are as below: The quantity of ERs and IRs is $K_E = 2$, $K_I = 2$, respectively. The initialization penalty factor is $\eta = 10^{-4}$. The accuracy of equation constraints is $\varepsilon_1 = 10^{-7}$. The convergence tolerance of the AO method is $\varepsilon_2 = 10^{-3}$. The maximum iterations count for the algorithm is $n_{\max} = 49$. The user noise power is $\sigma_i^2 = -120$ dBm. The scaling factor based on the penalty algorithm is $w = 10$. Assuming that all information receivers have the same QoS requirements, $\overline{R}_i = \overline{R}_0 \triangleq lb(1+\overline{\gamma}_0)$, $\overline{\gamma}_0$ is the minimal value of SINR required. The energy collection requirements for all energy receivers are $\overline{E}_j = \overline{E}_0 = 1$ mW.

The same simulation settings in the simulation analysis are listed in Table 2.

Figure 3 demonstrates the convergence of the method described in this paper. Among them, the quantity of intelligent reflector units is $M = 10$, and the quantity of transmitting antennas is $N = 2$. It can be observed that the iterative method in this paper guarantees the monotonicity of the minimized AP transmit power from Figure 3.

This paper tested three scenarios: SINR = 5 dB, SINR = 8 dB, and SINR = 10 dB. As the SINR increasing, the value to which the system converges gradually increases. This is because with the increase of SINR, higher requirements are placed on communication quality, and therefore, the required AP transmission power gradually increases. From Figure 3, it can also be seen that after two iterations, the convergence degree of the system

reaches about 90%. After three iterations, the AP transmission power tends towards a stable value, indicating that iterative method described in this paper is efficient.

**Table 2.** System Simulation Settings.

| Simulation Variables | Value |
|---|---|
| Quantity of information receivers | 2 |
| Quantity of energy receivers | 2 |
| Noise power | −120 dBm |
| Active STAR-RIS distance from AP | 10 m |
| Distance between IRs and active STAR-RIS | 20 m |
| Distance between ERs and active STAR-RIS | 2 m |

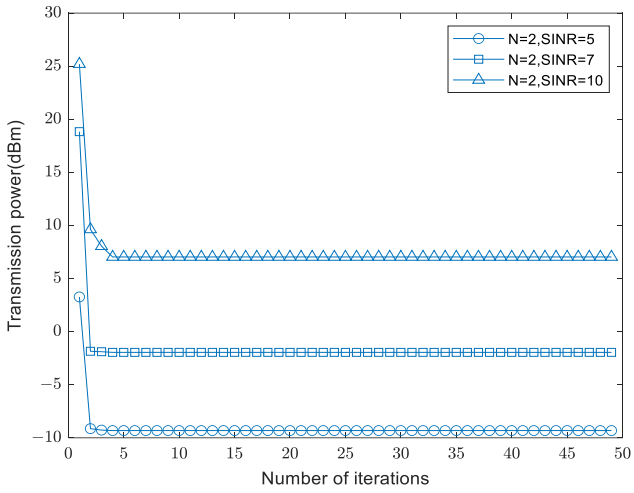


**Figure 3.** Algorithm Convergence.

Figure 4 shows how the AP transmission power changes with the change of the quantity of AP transmission antennas $N$ under five different models, where $M = 10$, and $\overline{\gamma}_0 = 10\,\text{dB}$. As observed in Figure 4, the AP transmission power assisted by active STAR-RIS is the lowest, while the AP transmission power assisted by passive RIS is the highest. This is because there is loss in the signal propagation process, while passive RIS can only reflect the signal and can only meet the minimum power requirements received by the energy receiver by increasing the AP transmission power. Active STAR-RIS can reflect accepted signals as well as transmit and amplify it, making full use of spectrum resources while reducing path loss, resulting in lower AP transmission power. From Figure 4, it can also be seen that when the passive beamforming variables $q_t$ and $q_r$ are taken as a random value, and only the active beamforming variable $\{w_i, v_j\}$ is optimized, the AP transmission power is greater than that of the active STAR-RIS. This is because when the passive beamforming variable is fixed, its coefficient matrix cannot be adjusted, and there is a lack of iterative optimization process. Additionally, as the quantity of transmitting antennas $N$ increases, AP transmission power of the five models gradually decreases. This is because more transmitting antennas mean that signals have more transmission paths; therefore, the AP transmission power gradually decreases.

Figure 5 shows the relationship between AP transmission power and the quantity of active STAR-RIS units $M$, where $N = 2$, and $\overline{\gamma}_0 = 10\,\text{dB}$. It can be observed that within a certain range, as the quantity of active STAR-RIS units increases, AP transmission power of five models gradually decreases from Figure 5. This is because, in one respect, when the quantity of active STAR-RIS units increases, active STAR-RIS has more degrees of freedom to achieve more reflection or transmission channels related to active STAR-RIS, achieving the effect of improving beamforming gain. In another respect, the more elements an active STAR-RIS has, the more paths and power it has to reflect or transmit

AP transmission signals, thus increasing the efficiency of the energy. However, as the quantity of active STAR-RIS units increases, the decreasing trend of AP transmission power gradually decreases. This indicates that within a certain range, increasing the quantity of active STAR-RIS elements is useful for the performance improvement of systems. When exceeding this range, the quantity of active STAR-RIS elements is no longer the key factor influencing AP transmission power. From Figure 5, it can also be seen that when the passive beamforming variables $q_t$ and $q_r$ are fixed, and only the active beamforming variables $\{w_i, v_j\}$ are optimized, the AP transmission power is highest compared to the other four models. This is because when the passive beamforming variables are fixed, the performance of RIS is not fully utilized. However, the other four models can be continuously optimized through iteration to achieve optimal performance. Therefore, the AP transmission power is maximized by fixing the passive beamforming variables and only optimizing the active beamforming variables.

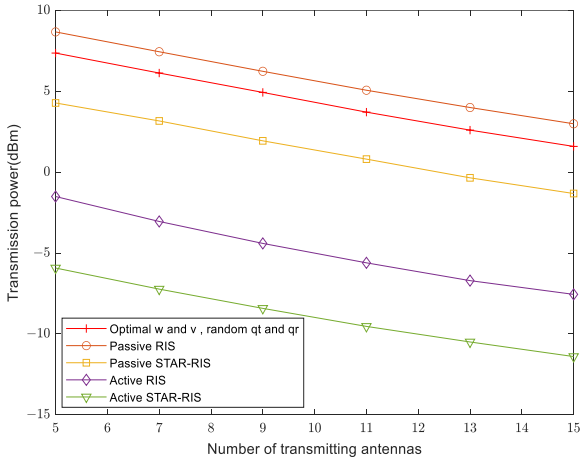


**Figure 4.** Relationship between AP transmission power and quantity of transmission antennas.

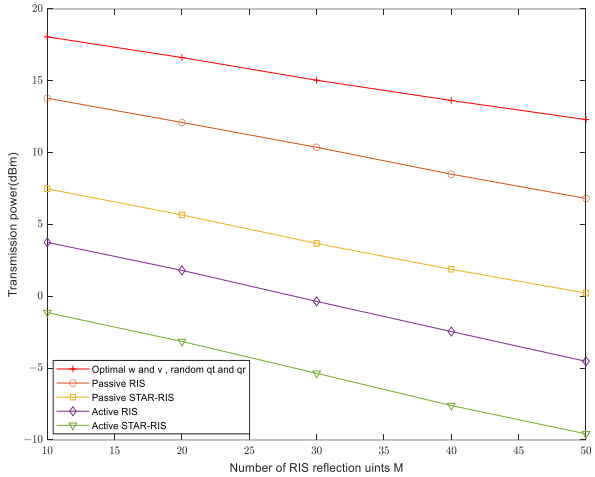


**Figure 5.** Relationship between AP transmission power and the quantity of active STAR-RIS units $M$.

Figure 6 presents how the power received by the minimum ERs changes with variations in the AP's transmission power, where $N = 2$, and $\overline{\gamma}_0 = 10$ dB. From Figure 6, it can be seen that in all four models, the AP transmission power gradually grows with the growth of the minimum power accepted by ERs. Among them, the AP transmission power demanded by systems with assistance of active STAR-RIS/RIS is generally smaller than that demanded by systems with assistance of passive STAR-RIS/RIS, and the AP transmission power demanded by systems with assistance of active STAR-RIS is the smallest. This is because active STAR-RIS and active RIS have a certain amplification effect on the signal, thereby reducing signal

attenuation, while passive STAR-RIS and passive RIS can only offset path loss by increasing AP transmission power, thereby meeting the minimum energy requirements received by the energy receiver. Compared to active RIS, active STAR-RIS not only reflects but also transmits signals, increasing the coverage range of signals sent by base stations. Even if the energy receiver is in a relatively poor channel environment and cannot receive the reflected signals, it can still receive signals transmitted from active STAR-RIS, improving the utilization of base station transmission signals and optimizing the efficiency of system operation.

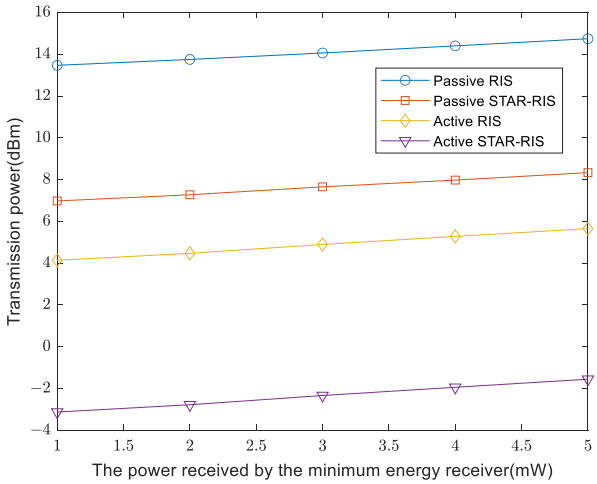


**Figure 6.** Relationship between AP transmission power and power received by minimum energy receiver.

As shown in Figure 7, the variation of AP transmission power with SINR value at the information receiver is shown, where $N = 2$, and $M = 10$. Similarly, we compare active/passive STAR-RIS and active/passive RIS. In Figure 7, as the SINR value increases, the AP transmission power of four models gradually increases. This is because the larger the SINR value at the IRs, the higher the required communication quality, thus requiring higher AP transmission power. From Figure 7, it can also be seen that the active STAR-RIS model proposed in this paper requires the smallest AP transmission power. This is because active STAR-RIS can reflect and amplify signals as well as transmit and amplify them, unlike passive RIS, thus making more use of frequency spectrum resources and reducing path loss. Although active RIS can amplify signals, it cannot transmit them. Although passive STAR-RIS can reflect and transmit signals, it cannot amplify them. Therefore, under the same conditions, the required AP transmission power is higher than active STAR-RIS.

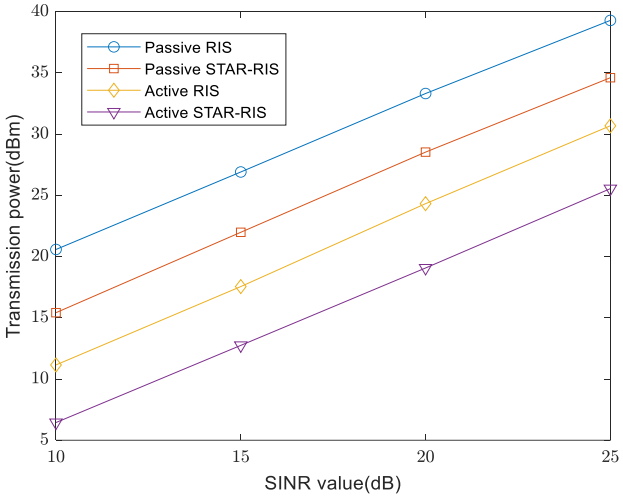


**Figure 7.** Relationship between AP transmission power and SINR value at the information receiver.

## 5. Conclusions

This paper researches an active STAR-RIS-assisted SWIPT system with a focus on minimizing transmission power from AP while satisfying communication rate and minimum energy collection requirements. The optimization strategy involves a joint tuning of the transmission precoding matrix, the reflection and transmission coefficient matrix, and the amplification matrix within the active STAR-RIS. The process begins by fixing the passive beamforming variables and applying SDR algorithm to determine the optimal active beamforming variables. Following this, the derived active beamforming variables are held constant, and a penalty-based algorithm is used to fine-tune the passive beamforming variables. This AO approach continues iteratively until the system reaches convergence. Compared to passive RIS, active RIS, and passive STAR-RIS configurations, the active STAR-RIS-assisted system provides substantial energy savings while maintaining consistent variables such as the quantity of transmitting antennas, the quantity of intelligent reflector units, the minimum power accepted by ERs, and the SINR at IRs. However, this paper only investigates the minimum transmission power of AP under perfect channel states and linear energy receiver models. In the future, we will study the problem of minimizing AP transmission power in more complex situations, such as in imperfect channel states and nonlinear energy receiver models.

**Author Contributions:** Conceptualization, C.G. and S.L.; methodology, C.G.; software, C.G.; validation, C.G., S.L. and M.W.; formal analysis, S.D.; investigation, Y.W.; resources, B.Y.; data curation, C.G.; writing—original draft preparation, C.G.; writing—review and editing, S.L.; visualization, S.L.; supervision, S.L.; project administration, S.L.; funding acquisition, S.L. All authors have read and agreed to the published version of the manuscript.

**Funding:** This work was supported in part by the Chunhui plan international cooperation project of China Education Ministry under Grant 202201406 and Grant HZKY20220171, in part by the key research and development plan of Xuzhou under Grant KC23134 and Grant KC22083, and in part by 2023 Jiangsu Graduate Practice Innovation plan under Grant SJCX23_1378.

**Data Availability Statement:** Please contact the corresponding author for the data in this paper because the data in the research involve intellectual property.

**Conflicts of Interest:** The authors declare no conflicts of interest.

## Appendix A

**Proof of Theorem 1.** The problem of relaxing $rank(W_i) = 1$ is jointly convex with respect to the optimization variables, and it satisfies Slater constraints; therefore, strong duality holds. To reveal the structure of $W_i$, the Lagrange function is given by the following equation:

$$\begin{aligned} L = &\sum_{i \in K_I} \mathrm{TR}(W_i) - \sum_{i \in K_I} \mathrm{TR}(Y_i W_i) + \mu_i(\overline{\gamma}_i \mathrm{TR}(H_{t,i} W_{\bar{i}}) - \mathrm{TR}(H_{t,i} W_{\mathrm{i}})) \\ &-\lambda_k(\sum_{k \in K_I} \mathrm{TR}(H_{r,j} W_k)) + \Delta \end{aligned} \tag{A1}$$

where $\Delta$ is the set of all items that do not depend on $\{W_i\}$; $\mu_i$, $\lambda_k$, and $Y_i$ are Lagrange multipliers related to constraints (10), (11), and (13), respectively. Based on the Karush–Kuhn–Tucker (KKT) condition regarding $W_i$, the optimal structure of $W_i^*$ can be characterized as follows:

$$\begin{aligned} &K1: \lambda_k^*, \mu_i^* \geq 0, Y_i^* \succeq 0 \\ &K2: Y_i^* W_i^* = 0_N \\ &K3: \nabla_{W_i^*} L = 0 \end{aligned} \tag{A2}$$

Among them, $\lambda_k^*$, $\mu_i^*$, and $Y_i^*$ represent the optimal Lagrange multiplier; $0_N$ represents the $N$-th order zero matrix; and $\nabla_{W_i^*} L$ is the gradient of $L$ with respect to $W_i^*$. $\nabla_{W_i^*} L$ can be represented as follows:

$$Y_i^* = I_N + \mu_i^*(\overline{\gamma}_i H_{t,i} - H_{t,i}) - \lambda_k^* H_{r,i} \tag{A3}$$

Using the results in Appendix A of reference [34], it can be proven that $rank(Y_i^*) = N - 1$. Furthermore, equation K2 means $rank(Y_i^*) + rank(W_i^*) \leq N$; therefore, $rank(W_i^*) \leq 1$ is established. Due to the service quality constraint in (10), the proof is complete for the optimal solution $rank(W_i^*) = 1$. Relaxing the rank constraint of $rank(V_j) = 1$ proves the same principle. □

## References


1. Wu, Q.; Li, G.Y.; Chen, W.; Ng, D.W.K.; Schober, R. An Overview of Sustainable Green 5G Networks. *IEEE Wirel. Commun.* **2017**, *24*, 72–80. [CrossRef]
2. Tombaz, S.; Vastberg, A.; Zander, J. Energy- and cost-efficient ultra-high-capacity wireless access. *IEEE Wirel. Commun.* **2011**, *18*, 18–24. [CrossRef]
3. Jameel, F.; Faisal; Haider, M.A.A.; Butt, A.A. A technical review of simultaneous wireless information and power transfer (SWIPT). In Proceedings of the 2017 International Symposium on Recent Advances in Electrical Engineering (RAEE), Islamabad, Pakistan, 24–26 October 2017; pp. 1–6.
4. Ozyurt, S.; Coskun, A.F.; Buyukcorak, S.; Karabulut Kurt, G.; Kucur, O. A Survey on Multiuser SWIPT Communications for 5G+. *IEEE Access* **2022**, *10*, 109814–109849. [CrossRef]
5. Li, S.; Gao, C.; Wei, M.; Zhao, J.; Shao, P.; Xu, J. CSI-Impaired Secure Resource Allocation for SWIPT-Enabled Full-Duplex Consumer Internet of Things Networks in Smart Healthcare. *IEEE Trans. Consum. Electron.* **2023**, *69*, 685–696. [CrossRef]
6. Liu, Y.; Liu, X.; Mu, X.; Hou, T.; Xu, J.; Di Renzo, M.; Al-Dhahir, N. Reconfigurable Intelligent Surfaces: Principles and Opportunities. *IEEE Commun. Surv. Tutor.* **2021**, *23*, 1546–1577. [CrossRef]
7. Mohamed, A.; Zappone, A.; Di Renzo, M. Bi-Objective Optimization of Information Rate and Harvested Power in RIS-Aided SWIPT Systems. *IEEE Wirel. Commun. Lett.* **2022**, *11*, 2195–2199. [CrossRef]
8. Yang, Z.; Zhang, Y. Optimal SWIPT in RIS-Aided MIMO Networks. *IEEE Access* **2021**, *9*, 112552–112560. [CrossRef]
9. Liu, Q.; Lu, M.; Li, N.; Li, M.; Li, F.; Zhang, Z. Joint Beamforming and Power Splitting Optimization for RIS-Assited Cooperative SWIPT NOMA Systems. In Proceedings of the 2022 IEEE Wireless Communications and Networking Conference (WCNC), Austin, TX, USA, 10–13 April 2022; pp. 351–356.
10. Zhou, G.; Pan, C.; Ren, H.; Zhi, K.; Hong, S.; Chai, K.K. User Cooperation for RIS-aided Secure SWIPT MIMO Systems under the passive eavesdropping. In Proceedings of the 2021 IEEE/CIC International Conference on Communications in China (ICCC Workshops), Xiamen, China, 28–30 July 2021; pp. 171–176.
11. Peng, H.; Wang, L.-C. Energy Harvesting Reconfigurable Intelligent Surface for UAV Based on Robust Deep Reinforcement Learning. *IEEE Trans. Wirel. Commun.* **2023**, *22*, 6826–6838. [CrossRef]
12. Li, S.; Wu, Y.; Zhang, Y.; Duan, S.; Xu, J.; Li, C. Privacy Transmission via Joint Active and Passive Beamforming Optimization for RIS-Aided NOMA-IoMT Networks. *IEEE Trans. Consum. Electron.* **2024**, *70*, 2290–2302. [CrossRef]
13. Zhi, K.; Pan, C.; Ren, H.; Chai, K.K.; Elkashlan, M. Active RIS Versus Passive RIS: Which is Superior With the Same Power Budget? *IEEE Commun. Lett.* **2022**, *26*, 1150–1154. [CrossRef]
14. Ren, H.; Chen, Z.; Hu, G.; Peng, Z.; Pan, C.; Wang, J. Transmission Design for Active RIS-Aided Simultaneous Wireless Information and Power Transfer. *IEEE Wirel. Commun. Lett.* **2023**, *12*, 600–604. [CrossRef]
15. Peng, Z.; Zhang, Z.; Pan, C.; Di Renzo, M.; Dobre, O.A.; Wang, J. Beamforming Optimization for Active RIS-Aided Multiuser Communications with Hardware Impairments. *IEEE Trans. Wirel. Commun.* **2024**. *early access*. [CrossRef]
16. Ma, Y.; Li, M.; Liu, Y.; Wu, Q.; Liu, Q. Active Reconfigurable Intelligent Surface for Energy Efficiency in MU-MISO Systems. *IEEE Trans. Veh. Technol.* **2023**, *72*, 4103–4107. [CrossRef]
17. Dong, L.; Yan, W. Active Reconfigurable Intelligent Surface (RIS) Aided Secure Wireless Transmission Under a Shared Power Source Between Transmitter and RIS. In Proceedings of the 2022 14th International Conference on Wireless Communications and Signal Processing (WCSP), Nanjing, China, 1–3 November 2022; pp. 996–1000.
18. Yaswanth, J.; Katwe, M.; Singh, K.; Prakriya, S.; Pan, C. Robust Beamforming Design for Active-RIS Aided MIMO SWIPT Communication System: A Power Minimization Approach. *IEEE Trans. Wirel. Commun.* **2024**, *23*, 4767–4785. [CrossRef]
19. Ahmed, M.; Wahid, A.; Laique, S.S.; Khan, W.U.; Ihsan, A.; Xu, F.; Chatzinotas, S.; Han, Z. A Survey on STAR-RIS: Use Cases, Recent Advances, and Future Research Challenges. *IEEE Internet Things J.* **2023**, *10*, 14689–14711. [CrossRef]
20. Wang, T.; Fang, F.; Ding, Z. Joint Phase Shift and Beamforming Design in a Multi-User MISO STAR-RIS Assisted Downlink NOMA Network. *IEEE Trans. Veh. Technol.* **2023**, *72*, 9031–9043. [CrossRef]
21. Zhao, P.; Zuo, J.; Wen, C. Power Allocation and Beamforming Vectors Optimization in STAR-RIS Assisted SWIPT. In Proceedings of the 2022 IEEE 22nd International Conference on Communication Technology (ICCT), Nanjing, China, 11–14 November 2022; pp. 1174–1178.
22. Zhu, G.; Mu, X.; Guo, L.; Huang, A.; Xu, S. Robust Beamforming Design for STAR-RIS Assisted SWIPT Systems. In Proceedings of the ICC 2023—IEEE International Conference on Communications, Rome, Italy, 28 May–1 June 2023; pp. 2123–2128.
23. Zargari, S.; Hakimi, A.; Tellambura, C.; Herath, S. Multiuser MISO PS-SWIPT Systems: Active or Passive RIS? *IEEE Wirel. Commun. Lett.* **2022**, *11*, 1920–1924. [CrossRef]
24. Boyd, S.; Vandenberghe, L.; Faybusovich, L. Convex Optimization. *IEEE Trans. Autom. Control.* **2006**, *51*, 1859.

25. Zhou, G.; Pan, C.; Ren, H.; Wang, K.; Nallanathan, A. A Framework of Robust Transmission Design for IRS-Aided MISO Communications with Imperfect Cascaded Channels. *IEEE Trans. Signal Process.* **2020**, *68*, 5092–5106. [CrossRef]
26. Papazafeiropoulos, A.; Elbir, A.M.; Kourtessis, P.; Krikidis, I.; Chatzinotas, S. Cooperative RIS and STAR-RIS assisted mMIMO communication: Analysis and optimization. *IEEE Trans. Veh. Technol.* **2023**, *72*, 11975–11989. [CrossRef]
27. Yu, X.; Sun, Q.; Chen, X.; Zhang, J.; Xu, C.; Yang, Y. Spectral Efficiency Analysis for RISs-Aided Wireless-Powered Cell-Free Massive MIMO. In Proceedings of the 2024 IEEE Wireless Communications and Networking Conference (WCNC), Dubai, United Arab Emirates, 21–24 April 2024; pp. 1–6.
28. Zhou, G.; Pan, C.; Ren, H.; Xu, D.; Zhang, Z.; Wang, J.; Schober, R. A framework for transmission design for active RIS-aided communication with partial CSI. *IEEE Trans. Wirel. Commun.* **2023**, *23*, 305–320. [CrossRef]
29. Ma, X.; Fang, Y.; Zhang, H.; Guo, S.; Yuan, D. Cooperative beamforming design for multiple RIS-assisted communication systems. *IEEE Trans. Wirel. Commun.* **2022**, *21*, 10949–10963. [CrossRef]
30. Cai, C.; Yuan, X.; Zhang, Y.J.A. RIS partitioning based scalable beamforming design for large-scale MIMO: Asymptotic analysis and optimization. *IEEE Trans. Wirel. Commun.* **2023**, *22*, 6061–6077. [CrossRef]
31. Li, W.; Wang, M.; Zhu, H.; Tian, Y. RIS Selection and Design over Computable Channels in Massive MIMO mmWave Systems. *IEEE Trans. Commun.* **2024**. *early access*. [CrossRef]
32. Peng, Z.; Chen, X.; Pan, C.; Elkashlan, M.; Wang, J. Performance analysis and optimization for RIS-assisted multi-user massive MIMO systems with imperfect hardware. *IEEE Trans. Veh. Technol.* **2022**, *71*, 11786–11802. [CrossRef]
33. Singh, S.; Raviteja, A.; Singh, K.; Singh, S.K.; Kaushik, A.; Ku, M.L. Secrecy Rate Maximization for Active RIS-Aided Robust Uplink NOMA Communications. *IEEE Wirel. Commun. Lett.* **2024**. *early access*. [CrossRef]
34. Xu, J.; Liu, L.; Zhang, R. Multiuser MISO Beamforming for Simultaneous Wireless Information and Power Transfer. *IEEE Trans. Signal Process.* **2014**, *62*, 4798–4810. [CrossRef]